

A CAMERA CALIBRATION ALGORITHM FOR THE UNDERWATER MOTION ANALYSIS

Young-Hoo Kwon
Ball State University, Muncie, Indiana, USA

A new camera calibration algorithm was developed through hybridisation of a geometric refraction-correction procedure and the 2D DLT method. For evaluation, the calibration errors in the image-plane coordinates were computed and compared with those obtained from the 3D DLT method in a simulated calibration trial. It was concluded that the new algorithm has potential advantages over the 3D DLT method in terms of the maximum calibration error and the extrapolation error.

KEY WORDS: underwater motion analysis, camera calibration algorithm, refraction, DLT method

INTRODUCTION: One major obstacle encountered in the underwater motion analysis is the error caused by light refraction. Regardless of the system involved in recording, such as waterproof camera housing, inverse periscope, and underwater viewing window, there always is a water-(glass)-air interface involved and refraction occurs at the interface.

Several investigators have attempted underwater motion analyses using the DLT method (Abdel-Aziz and Karara, 1971) in the camera calibration, including Cappaert, Pease and Troup (1995) and Kwon and Sung (1995). Since refraction **distorts** the collinearity condition that the DLT method is based upon, the object-space coordinates of the control points are forced to fit to erroneous (refracted) image-plane coordinates during the camera calibration and the mismatching error must be distributed throughout the entire control volume. Kwon (1998) investigated the object-plane deformation problem due to refraction in the underwater motion analysis using the 2D DLT method.

Since the geometry of the underwater motion analysis is fairly complex, few alternative methods have been reported. The purpose of this study was to develop a new camera calibration method with refraction-correction capability and to test it through comparison with the 3D DLT method, the commonly used calibration method in the underwater motion analysis.

METHODS:

Geometry of the Underwater Motion Analysis: Figure 1 summarises the geometry of the underwater motion analysis with three reference frames defined: the object-space reference frame (XYZ-system; frame S), the interface-plane reference frame (X'Y'Z'-system; frame F) and the image-plane reference frame (UVW-system; frame I). Frame F was defined in such a way that its origin is located at point O' (the projection of point N on plane I) and axis Y' is drawn toward point O_F (projection of point O on plane F). Point N is the node point (projection centre) of the camera while axis X' is the symmetry axis that is perpendicular to plane F. The thickness of the interface (glass) was ignored throughout this study.

Point M shown in Figure 1 is a marker (control point) while point I is its corresponding image point. Point R is the refraction point (the intersection of the refracted ray with plane F) and points R, I and N are collinear. Point P, projection of point N on plane I, is the principal point of plane I while the distance **between** points N and P is the principal distance.

In under-water filming, a total of 12 experimental factors can be identified: the node-to-interface distance (D_N shown in Figure 1), the calibration frame to interface distance (D_X), the symmetry-axis-to-calibration-frame distance (D_Y), three Eulerian angles (Φ_1 , Φ_2 and Φ_3) which characterize the relative orientation of frame F to frame S, and six camera parameters such as the principal distance (D_I), the U and V coordinates of the principal point (u_o and v_o), and three Eulerian angles (Θ_1 , Θ_2 and Θ_3) which characterize the relative orientation of frame I to frame F. Therefore, the F-frame coordinates of a control point (x' , y'

and z') can be computed from its S-frame coordinates (x, y and z):

$$\begin{pmatrix} x' \\ y' \\ z' \end{pmatrix} = \begin{pmatrix} c(\Phi_3) & 0 & -s(\Phi_3) & 1 & 0 & 0 \\ 0 & 1 & 0 & 0 & c(\Phi_2) & s(\Phi_2) \\ s(\Phi_3) & 0 & c(\Phi_3) & 0 & -s(\Phi_2) & c(\Phi_2) \end{pmatrix} \begin{pmatrix} c(\Phi_1) & s(\Phi_1) & 0 \\ -s(\Phi_1) & c(\Phi_1) & 0 \\ 0 & 0 & 1 \end{pmatrix} \begin{pmatrix} x \\ y \\ z \end{pmatrix} + \begin{pmatrix} -D_X \\ D_Y \\ 0 \end{pmatrix} \quad (1)$$

where $c() = \cos$, and $s() = \sin$.

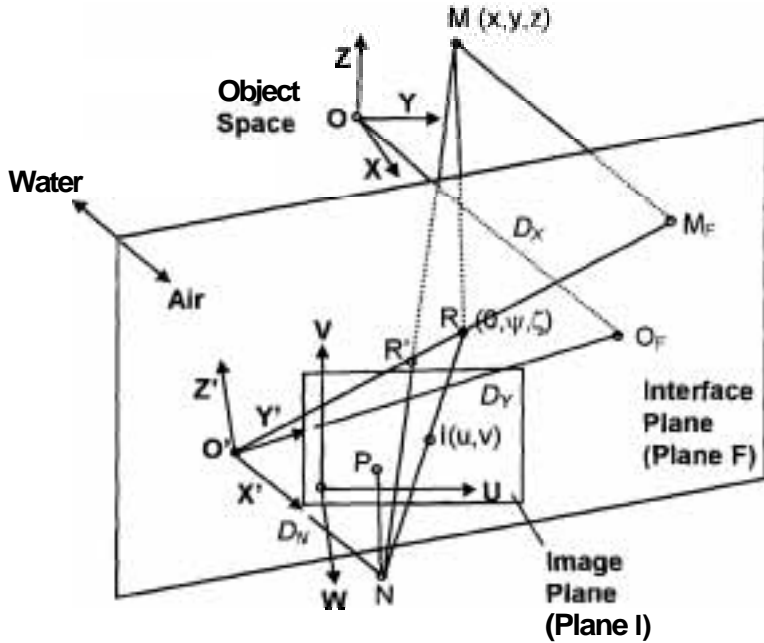


Figure 1 - Geometry of the underwater motion analysis

Calibration Algorithm: A new camera-calibration algorithm was developed through hybridisation of a geometric refraction-correction procedure and the 2D DLT method. The geometric refraction-correction procedure was formulated based on the Snell's law of refraction for the computation of the F-frame coordinates of the refraction point (point R): ψ and ζ shown in Figure 1. A refraction index of 1.3330 was used in this process for the water-air interface. Basically, the F-frame coordinates of the refraction point were expressed as:

$$(\theta, \psi, \zeta)^T = k \cdot (\theta, y', z')^T \quad (2)$$

where $k =$ a scalar ratio computed from the M -to- M_F distance, O' -to- M_F distance and D_N , and $()^T =$ transpose of $()$.

The 2D DLT method (Walton, 1981) was incorporated in the algorithm for the elimination of the camera parameters (D_N , ψ , γ , Θ_1 , Θ_2 and Θ_3) from the model. This is possible since points R, I and N are collinear. Given accurate estimation of the 6 remaining distance and angle factors (Φ_1 , Φ_2 , Φ_3 , D_N , D_X and D_Y), the F-frame coordinates of the refraction points can be obtained from equations 1 and 2. Then, the refraction-point coordinates (ψ and ζ) can be directly transformed to the image-plane coordinates (u and v) using the 2D DLT equations:

$$u = \frac{L_1 \cdot \psi + L_2 \cdot \zeta + L_3}{L_7 \cdot \psi + L_8 \cdot \zeta + 1}, \quad v = \frac{L_4 \cdot \psi + L_5 \cdot \zeta + L_6}{L_7 \cdot \psi + L_8 \cdot \zeta + 1} \quad (3)$$

where L_1 to $L_8 =$ DLT parameters (combinations of the camera parameters and D_N). It is much simpler to compute the eight DLT parameters than the six camera parameters.

Testing of the Algorithm: The new calibration algorithm was evaluated through comparison with the 3D DLT method. Instead of an actual experiment, the comparison was performed based on a simulated calibration trial to eliminate any unnecessary contamination of the data. An imaginary calibration frame (2 m wide, 2 m high and 4 m long)

was designed and a total of 45 control points were distributed evenly throughout the control volume with the distance between the adjacent points being 1 m. A set of simulated I-plane coordinates of the control points were generated from the geometric relationship shown in Figure 1:

$$\begin{pmatrix} \xi' \\ \psi' \\ \zeta' \end{pmatrix} = \begin{pmatrix} c(\Theta_3) & s(\Theta_3) & 0 \\ -s(\Theta_3) & c(\Theta_3) & 0 \\ 0 & 0 & 1 \end{pmatrix} \begin{pmatrix} c(\Theta_2) & 0 & -s(\Theta_2) \\ 0 & 1 & 0 \\ s(\Theta_2) & 0 & c(\Theta_2) \end{pmatrix} \begin{pmatrix} 1 & 0 & 0 \\ 0 & c(\Theta_1) & s(\Theta_1) \\ 0 & -s(\Theta_1) & c(\Theta_1) \end{pmatrix} \begin{pmatrix} -D_N \\ \psi \\ \xi \end{pmatrix} \quad (4)$$

$$\begin{pmatrix} u \\ v \end{pmatrix} = -\frac{D_I}{\xi'} \begin{pmatrix} \psi' \\ \zeta' \end{pmatrix}$$

where $(\xi', \psi', \zeta')^T$ = vector NR described in frame I. Here, an arbitrary set of experimental factors were used: $D_N = 0.5$ m, $D_X = 7$ m, $D_Y = 1$ m, $\Phi_1 = \Phi_2 = \Phi_3 = 0^\circ$, $D_I = 1$ m, $u_0 = v_0 = 0$ DU, and $\Theta_1 = \Theta_2 = \Theta_3 = 0^\circ$. Note that the unit of u and v is an arbitrary digitising unit (DU). After the camera calibration, the I-plane coordinates (u and v) of the control points were reconstructed for the assessment of the calibration error (ϵ):

$$\epsilon = \sqrt{\Delta u^2 + \Delta v^2} \quad (5)$$

where $\Delta u = u - \frac{L_1\psi + L_2\zeta + L_3}{L_7\psi + L_8\zeta + 1}$, and $\Delta v = v - \frac{L_4\psi + L_5\zeta + L_6}{L_7\psi + L_8\zeta + 1}$. Similar approach was also used

for the 3D DLT method. The root-mean-square (RMS) and maximum calibration errors were computed for comparison. In addition, a total of 12 points were placed outside the control volume (1 m away from the control volume) for the assessment of the extrapolation error.

A Visual C++ program (**Uw3D.EXE**) was developed and used in generation of the simulated U and V coordinates, in calibration, and in computation of the errors.

RESULTS AND DISCUSSION: Table 1 summarises the results of the camera calibration. The new method successfully reconstructed the I-plane coordinates of the control points. Since the same distance and angle factors ($D_N = 0.5$ m, $D_X = 7$ m, $D_Y = 1$ m, and $\Phi_1 = \Phi_2 = \Phi_3 = 0^\circ$) were used in both generation of the simulated I-plane coordinates and calibration, this results suggest that the hybridisation of the geometric refraction-correction procedure and the 2D DLT method was working well as expected. The maximum extrapolation error from the 12 extra points placed outside the control volume (1 m away from the boundary) also proved an accurate extrapolation of the coordinates.

Table 1 Calibration Results (Unit: DU)

	Mean error	Max. error	Max. extrapolation error
New method	2.90×10^{-5}	5.00×10^{-5}	4.36×10^{-4}
3D DLT method	0.57×10^0	1.38×10^0	5.00×10^0

The 3D DLT method, on the other hand, generally scored much larger calibration errors than the new method did. Considering the maximum range of the u coordinates, a maximum error of 1.38 DU was equivalent to a real-life length of approximately 5.75 cm. The maximum extrapolation error observed in the 3D DLT calibration in turn was equivalent to 18.18 cm. Moreover, these real-life error estimations are based on one camera and adding more cameras in a 3D analysis will inevitably enlarge the overall error. In other words, the main problem in applying the 3D DLT method in the underwater motion analysis is the large maximum errors at the boundary of the control volume and even larger extrapolation errors. This justifies the effort to develop a new camera-calibration method with refraction-correction capability.

According to Kwon (1998), decrease in the interface-to-node-point distance (D_N shown in Figure 1) or the calibration-frame-to-interface distance (D_X) causes a sharp increase in the calibration error. Since the waterproof housing system generally provides the shortest D_N

and D_x among the underwater recording systems, the error due to the intrinsic problems of the 3D DLT method can be fatal in spite of its flexibility in terms of camera positioning. Cappaert et al. (1995) attempted motion analysis of Olympic swimmers using waterproof underwater cameras but without reporting the RMS and maximum calibration errors. These investigators computed the location of the shoulder joint twice, once from the underwater views and once from the over-water views, and forced the two sets of coordinates to fit to each other by translating the coordinates obtained from the underwater views. This approach seemed to be a result of the discontinuity in the object space due to large object space deformation. Moreover, simple translation can not solve the space deformation error due to refraction.

The new method is based on the assumption that the distance and angle factors are accurate. In other words, an inaccurate estimation of the distance and angle factors may cause an overall inaccurate camera calibration. In order to assess the problems associated with an inaccurate estimation of the experimental factors, the distance and angle factors were intentionally perturbed within 5 cm and 5° range with the steps being 1 cm and 1°, respectively. The angle factors were perturbed separately from the distance factors. In the distance-factor perturbation, the maximum values of the maximum and maximum extrapolation errors from the 1331 sets of calibrations were 0.51 DU and 0.77 DU, respectively. The maximum values from the angle-factor perturbation calibration sets (N = 1331) were 4.83 DU and 7.45 DU, respectively. In other words, the calibration error is more sensitive to the errors in the angle factors than to those in the distance factors.

Given relatively close initial estimation of the distance and angle factors, one may develop an optimisation strategy that involves multi-level systematic perturbations of the distance and angle factors. Incorporation of this kind of optimisation strategy in the algorithm will enhance the applicability of the new calibration method.

CONCLUSION: It was concluded through a comparison with the 2D DLT method that the new method has potential advantages over the 3D DLT method in terms of the maximum calibration error observed at the border of the control volume and the extrapolation error. Addition of an optimisation strategy for the distance and angle factors will enhance this new algorithm.

REFERENCES:

- Abdel-Aziz, Y.I., & Karara, H.M. (1971). Direct linear transformation from comparator coordinates into object space coordinates in close-range photogrammetry. In *Proceedings of the Symposium on Close-Range Photogrammetry*. Falls Church, VA: American Society of Photogrammetry.
- Cappaert, J.M., Pease, D.L., & Troup, J.P. (1995). Three Dimensional analysis of the men's 100-m freestyle during the 1992 Olympic Games. *Journal of Applied Biomechanics*, 11, 109-112.
- Kwon, Y.-H. (1998). Object plane deformation due to refraction in 2-Dimensional underwater motion analysis. *Journal of Applied Biomechanics* (accepted).
- Kwon, Y.-H., & Sung, R.-J. (1995). A comparative biomechanical evaluation of the start techniques of selected Korean national swimmers. *Korean Journal of Sport Science*, 7, 22-34.
- Walton, J.S. (1981). *Close-range cine-photogrammetry: a generalized technique for quantifying gross human motion*. Ph.D. dissertation, Pennsylvania State University.